Dielectric and high-pressure investigations on a thermotropic cubic mesophase

D. S. Shankar Rao, S. Krishna Prasad, Veena Prasad, and Sandeep Kumar
Centre for Liquid Crystal Research, Jalahalli, Bangalore 560 013, India
(Received 20 November 1998)

Optically isotropic cubic mesophases, which are commonly exhibited by lyotropic materials, have been observed in a few thermotropic liquid crystalline systems also. Although the first thermotropic cubic mesophase was reported about 40 years ago, its existence in diverse systems is only a recent finding. Moreover, the investigations on this mesophase have mainly concentrated on the structural aspects. While the effect of pressure has not been reported, only one dielectric measurement seems to have been carried out. In this paper we present the results of our dielectric and high pressure investigations on a compound exhibiting a thermotropic cubic mesophase. Two salient results are (i) a low frequency relaxation mode is observed with a large dielectric strength with appreciable changes across the columnar-cubic and cubic-smectic *C* transitions; and (ii) the cubic phase ceases to exist when the applied pressure exceeds about 400 bar. [S1063-651X(99)14705-6]

PACS number(s): 61.30.−v, 64.70.Md, 77.84.Nh

INTRODUCTION

Liquid crystals [1] are often referred to as anisotropic fluids. However, optically isotropic cubic mesophases are known to occur in some thermotropic systems and more commonly in lyotropic systems [2]. In lyotropic materials the different chemical nature of the two parts of the molecules, viz., the hydrophilic polar head groups and the hydrophobic alkyl tails lead to the formation of micelles, which in turn can arrange themselves to give cubic structure. These cubic phases occur either between the lamellar and hexagonal columnar phases or between the hexagonal columnar phase and the isotropic micellar solution. Also, depending on the value of the interface curvature between the hydrophilic and hydrophobic regions, they can be the normal or inverted type.

In contrast to the wealth of knowledge available on lyotropic materials, not much is known about cubic mesophases in thermotropic systems. The main reason has been that only very few cases of thermotropic cubic phases were known till recently [3,4]. However, the finding of these mesophases in diverse thermotropic systems in the last few years has led to a spurt of activity in this field [5]. The dielectric properties of the thermotropic cubic phases have not been well studied; in fact, to our knowledge, there has been only one such study reported recently [6]. Further, no measurements on the effect of pressure seem to have been carried out. In this paper we present dielectric dispersion measurements and the pressure-temperature phase diagram of a compound exhibiting a thermotropic cubic mesophase. Moreover, this compound shows a smectic-cubic-columnar phase sequence, which is very similar to the lamellar-cubic-hexagonal columnar sequence observed in lyotropic systems.

EXPERIMENT

The structural formula of the investigated compound, 4′-hexadecyloxy-3′-nitro biphenyl carboxylic acid, is shown below.

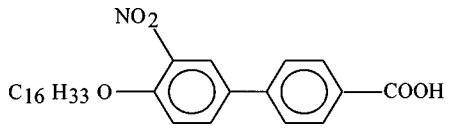

The transition temperatures (in °C) and enthalpies (in J/g and enclosed in parentheses) obtained in the heating and cooling modes using optical microscopy in conjunction with a programmable hot stage (Mettler FP90) and a differential scanning calorimeter (Perkin Elmer DSC7), are given below.

Heating mode:

$$\text{smectic } C \xrightarrow{176.4\ (1.29)} \text{cubic} \xrightarrow{198.7\ (3.05)} \text{smectic } A \xrightarrow{200.5\ (2.16)} \text{isotropic}$$

Cooling mode:

$$\text{isotropic} \xrightarrow{200.1\ (1.9)} \text{smectic } A \xrightarrow{194.2\ (1.10)} \text{columnar} \xrightarrow{192.9\ (0.75)} \text{cubic} \xrightarrow{162.5\ (1.33)} \text{smectic } C.$$

The hystereses in the transition temperatures, especially for the smectic *C* (Sm*C*)-cubic transition, and the appearance of the columnar (col) phase in the cooling mode have been reported earlier [3,7,8]. Further the range and the actual temperature of the transitions involving the col phase were found to be dependent on factors like thickness of the sample and cooling rate. We have followed a slightly different synthetic route than is traditionally used [9]. The *o*-alkylated ethyl ester of the starting material 4′-hydroxy-4-biphenyl carboxylic acid was subjected to nitration and the product was hydrolyzed to get the required compound, which was purified by repeated recrystallization. Care was taken to confirm the structures of all the intermediates and the final compound using IR and ^{1}H NMR spectroscopy. In our opinion, the advantage of this procedure over the traditional method of Gray, Jones, and Marson [9] is the following. In our method the presence of the bromo intermediate in the final product, a known source of contamination in the traditional route, and which particularly affects the stability of the col phase, is completely eliminated.

Dielectric experiments were done using a frequency response analyzer (Solatron 1260) in the frequency range 1 Hz to 100 kHz and a probing voltage of 500 mV. The sample was sandwiched between two indium tin oxide (ITO) coated glass plates with mylar spacers to define the cell thickness ($\sim$25 μm). The sample temperature was varied using a programmable hot stage (Mettler FP90) and was precisely measured using a calibrated thermistor placed very close to the sample cell. The data collection was handled by a PC with the control routine written in the LABVIEW 4.0 environment. The dielectric dispersion curves were analyzed using a nonlinear equation-fitting program (WINFIT 2.3, Novocontrol GmBH).

Pressure studies were carried out using an optical high pressure cell, details of which are described in an earlier paper [10]. Essentially it consists of a sample sandwiched between optically polished sapphire rods enclosed in an elastomeric tube. A low-viscosity oil was used as the pressurizing medium. At different fixed pressures the intensity of a He-Ne laser beam transmitted through the sample was monitored as a function of temperature with the help of a photodiode with a built-in amplifier. The sample pressure was measured by employing a precision Heise gauge. A PC handled the data acquisition and control of the experiment.

RESULTS AND DISCUSSION

A. Differential scanning calorimetry

Figure 1 shows the differential scanning calorimeter scans taken in both the heating and cooling modes at a rate of 1 °C/min. The lowest temperature peak has been identified to correspond to the Sm*C*-cubic transition and the one at about 202 °C corresponds to the smectic *A* (Sm*A*)-isotropic transition. The cubic to Sm*A* transformation that appears as a broad peak in the heating mode is quite sharp in the cooling mode, and appears to have a single peak. However, when the cooling rate is reduced to 0.2 °C/min, two clear peaks are resolved (see inset of Fig. 1). Microscopic observations show that in the cooling cycle, the Sm*A* phase transforms to a

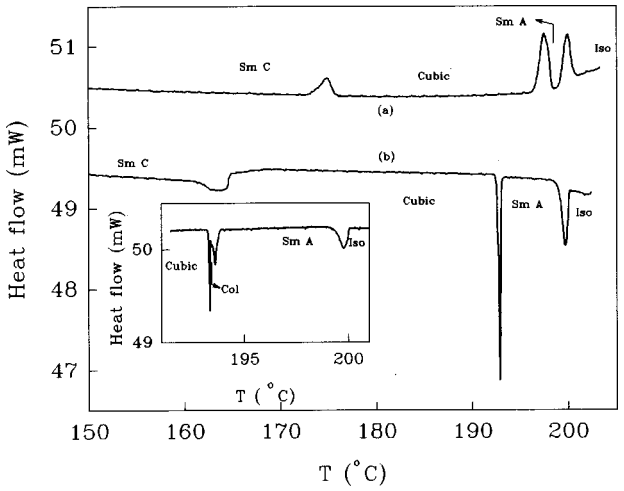

FIG. 1. Differential scanning calorimeter traces obtained in the (a) heating and (b) cooling modes at a rate of 1 °C/min. The significant difference in the transition temperatures, the peak onset temperature, between the heating and cooling modes is a known feature for the compound studied. The inset shows a scan taken at a cooling rate of 0.2 °C/min. Notice that an additional peak is seen just above the transition to the cubic phase. Comparing the texture obtained for the intermediate phase with literature reports, we identify this phase as a columnar (or col) phase. In fact, at the rate of cooling used for the scan shown in (b), we were not able to resolve this peak.

phase with mosaic texture which at a slightly lower temperature changes to the optically isotropic-cubic phase. However, in the heating mode the cubic phase goes directly to the Sm*A* phase. The intermediate phase, which has been identified in earlier reports as a columnar (col) phase [7,11], is thus a monotropic phase. As we mentioned earlier, owing to the absence of bromo impurities, we found that columnar phase is quite stable and could be held steady for extended periods of time, which enabled us to perform the first detailed study in this phase. The transition enthalpy values obtained by us for the different transitions are in quite good agreement with the data available in the literature [8,12].

B. Dielectric studies

Figure 2 shows a representative dielectric dispersion scan taken in the isotropic phase. The profiles obtained in the different mesophases were quite similar to this scan. A dielectric absorption peak with a relaxation frequency at about 160 Hz and a linear decrease of the ε'' value at low frequencies are observed, the latter variation being typical of frequency-dependent conductivity. We modeled such a combined process using the Havriliak-Negami mechanism [13] and a conductivity part and expressed the imaginary part of the dielectric constant as

$$\varepsilon''_{\text{measured}}(f) = \frac{\sigma}{2\pi\varepsilon_o f^m} + \text{Im}\left(\frac{\Delta\varepsilon}{\left\{ 1 + \left(i\frac{f}{f_R} \right)^{\alpha} \right\}^{\beta}} \right). \quad (1)$$

Here f is the measuring frequency, σ is the specific conductivity of the sample, ε_o is the vacuum permittivity, $\Delta\varepsilon$ and f_R

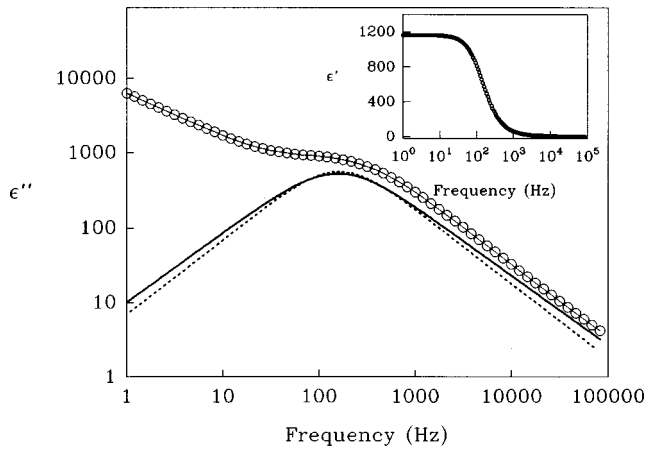

FIG. 2. Raw plot of imaginary part of the dielectric permittivity ε'' vs frequency in the isotropic phase. The experimental data are indicated by circles and the fitting to the Havriliak-Negami equation [Eq. (1)] by a thin solid line. The linear decrease in $\log \varepsilon''$ at low frequencies is attributed to conductivity contribution and the thick solid line shows the profile obtained after subtracting this contribution. For comparison, an ideal Debye relaxation profile [α, $\beta=1$ in Eq. (1)] is shown as a dashed line. The frequency dependence of the real part of the dielectric constant is shown in the inset.

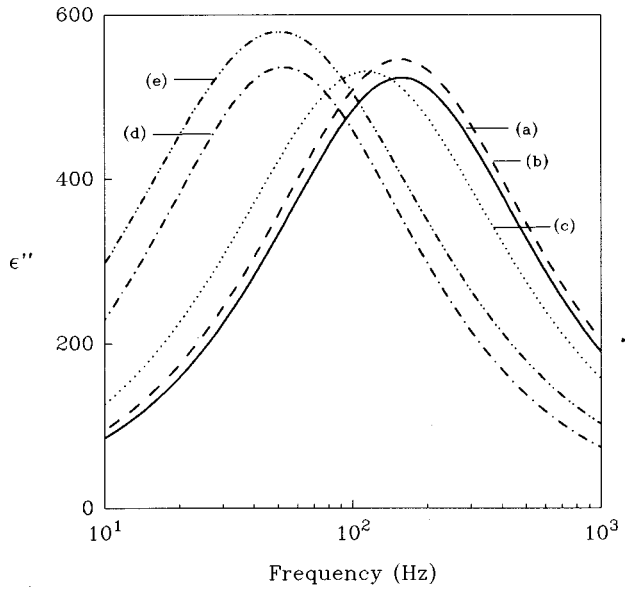

FIG. 3. Representative plots of ε'' vs frequency in the (a) isotropic (——), (b) Sm*A* (– –), (c) col (· · · ·), (d) cubic (— . — . — . —), and (e) Sm*C* (– · · –) phases. For the purpose of presentation, the raw data corrected for the conductivity contribution has been used. Notice a near-Debye type of profile in all the phases, which indicates that the distribution in the relaxation times is quite small. The remarkably low relaxation frequency, approximately the frequency corresponding to the peak position, is due to the extended hydrogen-bond network.

represent the dielectric strength and relaxation frequency of the mode under consideration. The parameters α and β describe the shape of ε'' versus f profile; $\alpha,\beta=1$ describes the shape for a Debye type of relaxation. We found that over the entire temperature range of measurement, the parameter β was equal to 1, indicating that the profiles are symmetric about the maximum in the dielectric loss factor. The parameter α was found to take a value between 0.85 and 0.95, signifying that the distribution of the relaxation times is quite narrow. In the temperature range of these measurements, the parameter m was in the range 0.7 to 0.9. The conductivity contribution is observed to be quite large, a feature that is in common with a diol compound studied by Kresse *et al.* [6]. It can be attributed to the presence of an extended network of hydrogen bonds even in the isotropic phase. Calorimetric [14] and IR [12] studies on this compound have shown that the hydrogen bonding does persist in the isotropic phase also.

As the interest is in the dielectric relaxation process, we have presented in Fig. 3 the ε'' versus f profiles obtained in the different mesophases, after subtracting out the conductivity contribution. The features that are interesting to note are (i) the overall change in the relaxation frequency between the different mesophases is quite small, (ii) the absolute value of f_R is quite low, and (iii) the amplitudes of the peaks are very large, much larger than usually observed for nonchiral liquid crystalline substances. Comparing with the dielectric results on diols [6] we observe that the relaxation frequency is about two orders of magnitude smaller and that the amplitude is larger by roughly the same amount. We will come back to the reasons for these observations later.

The detailed temperature variation of the relaxation frequency and the dielectric strength obtained on cooling the sample from the isotropic phase are shown in Fig. 4. Clear changes are seen at temperatures corresponding to all the transitions observed in the calorimetric and optical microscopic measurements. On cooling from the isotropic phase, the relaxation frequency decreases with decreasing temperature and reaches a minimum at the transition. Concomitant with this decrease in frequency, an increase in the dielectric strength, which is the amplitude of the mode, is observed. This type of a pretransitional slowing down of the relaxation frequency associated with the orientational ordering in the liquid crystalline phase is usually observed at the isotropic-

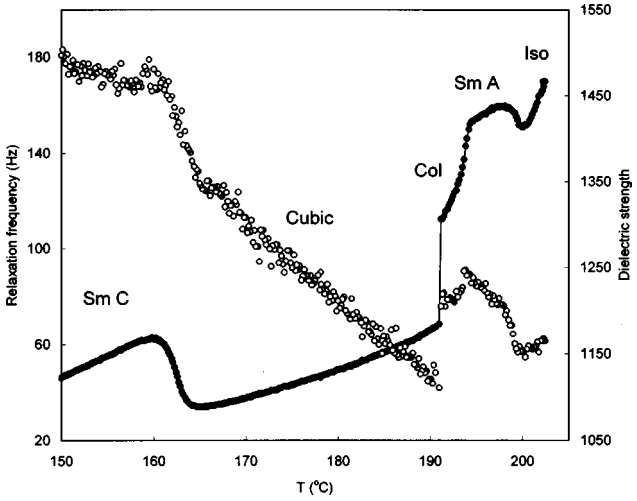

FIG. 4. Temperature dependence of the (●) relaxation frequency and (○) dielectric strength obtained from fitting the ε'' vs frequency data to Eq. (1). Clear changes are observed at temperatures corresponding to the different transitions. The line through the frequency data is meant to show the jump at the col to the cubic transition.

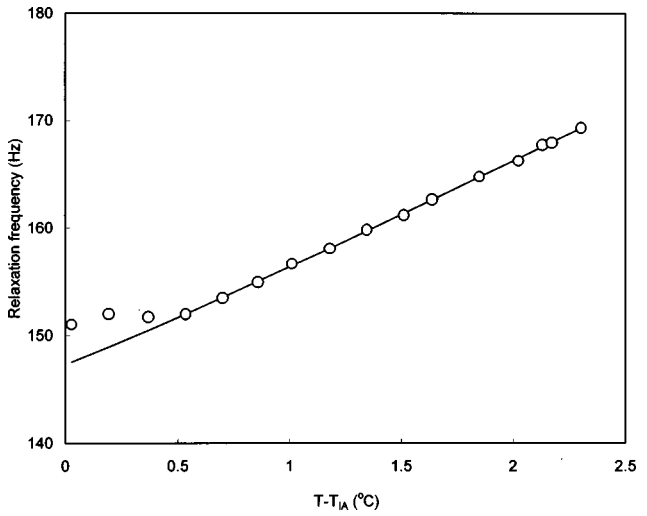

FIG. 5. Expanded plot showing the explicit variation of the relaxation frequency with reduced temperature in the isotropic phase in the vicinity of the transition to the Sm*A* phase. The circles represent the experimental data and the line shows a fit to a simple power-law with an exponent of 1.06 ± 0.1. This value is indicative of a mean-field type of behavior. The deviation of the data from the fit close to the transition is due to the first-order nature of the transition.

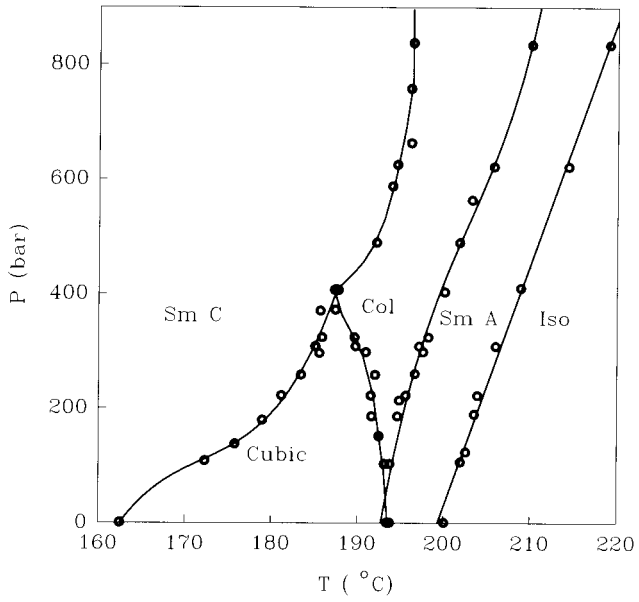

FIG. 6. Pressure-temperature phase diagram of the compound studied. A negative slope of the col-cubic transition not only stabilizes the col phase but also results in the bounding of the cubic phase at a pressure of about 400 bar. The open circles represent experimental data and the lines are meant as guides to the eye. The solid circle indicates the col-cubic-Sm*C* *three-phase* meeting point, which is likely to be a simple *triple point.*

nematic transition and seldom seen for the isotropic-Sm*A* transition [15]. This is because, generally the latter transition has a very large enthalpy and therefore a smaller associated pretransitional effect compared to the isotropic-nematic one. But as we saw earlier, the isotropic-Sm*A* transition enthalpy for the compound studied here is quite small and this possibly explains the observation of the pretransitional slowing down of the order parameter mode. Following the practice [15,16] of describing discontinuous transitions that exhibit strong pretransitional behavior using power-law expressions, we have tried a similar analysis for the temperature versus relaxation frequency data in the isotropic phase. This data, separately shown in Fig. 5, is fitted to a power law of the form $f_R \propto t^{\gamma}$, where $t=(T-T^*)$, T^* being the hypothetical second-order isotropic-Sm*A* transition temperature. The actual transition occurs at a temperature T_{IA}, slightly above T^*. A finite difference between T_{IA} and T^* would lead to a rounding of the data close to the transition. For this reason, the fitting was done by not including data from that region. The fit yields a value of $\gamma=1.1\pm0.1$, which within experimental errors, indicates a mean-field type of behavior and is similar to what is generally observed for the isotropic-nematic transition. Further, a rather small value of $T_{\mathrm{IA}}-T^*$ $(=0.5\,^{\circ}\mathrm{C})$ obtained is again comparable to the value usually observed for the isotropic-nematic transition. But as remarked earlier, the large value for the dielectric strength is due to the hydrogen bonding. Hence the usual mean-field type of behavior would perhaps indicate that the coupling between the orientational fluctuations of the molecules and the extended hydrogen bond network is quite strong.

While the Sm*A*-col transition also shows a strong pretransitional variation, the col-cubic transition is observed to be very abrupt. This perhaps is to be expected, as the former transition is from a 1D ordered phase to a 2D ordered one, whereas the latter is 2D ordered to an isotropic one. However, the cubic structure reduces the degree of freedom for the micelles to reorient and thus the frequency decreases at the col-cubic transition. This freedom is partially recovered at the transition to the Sm*C* phase as seen by an increase in the relaxation frequency. From a simplistic point of view, the degree of freedom can be estimated using the associated activation energy for the process. We have calculated this parameter using the expression, $f_R \propto \exp(-w/k_BT)$ with k_B, the Boltzmann constant and w, the activation energy. As the range of the Sm*A* and col phases are small, we have not calculated the values of w in these phases. For the isotropic, cubic and Sm*C* phase the values are 116.9 ± 3 kJ/mole, 45.6 ± 0.1 kJ/mole, and 51.7 ± 0.1 kJ/mole, respectively. It appears that the environment for the reorientation of the aggregates is only slightly different between the cubic and Sm*C* phases. The value in the cubic phase is higher than what is observed for the cubic phase of a diol compound, the only other instance for which data is available [6].

C. Pressure studies

Before describing the results, we would like to state one aspect of the experimentation here. As the compound is not chemically very stable, a fact that is well known, the overall pressure-temperature (P-T) diagram has been obtained using several cell mountings. In each of the mountings, after a few runs at higher pressures, the sample was brought down to room pressure to check for the stability of the compound. If the transition temperatures did not match with the values before applying the pressure, the runs were discarded. Figure 6 shows the P-T diagram and one can notice several interesting features. (a) The col phase, which is known to be a highly metastable phase at room pressure, not only gets sta-

bilized, but increases in its temperature range with pressure; the range which is only about 0.4 °C at atmospheric pressure increases to about 13.5 °C for a pressure of about 800 bar. This is due to the opposing features seen for the two other phase boundaries: while the Sm*A*-col phase line shows a positive slope with a dT/dP of 16.6 °C/kbar at 1 bar, the col-cubic boundary has a strong negative slope $[(dT/dP)_{1\ \mathrm{bar}} = -10.9\,^{\circ}\mathrm{C/kbar}]$. (b) The negative slope of the col-cubic boundary together with the positive slope for the cubic-Sm*C* line, leads to the cubic phase getting bound at about 400 bar, resulting in a col-cubic-Sm*C* three-phase meeting point. Since both col-cubic and cubic-Sm*C* transitions are first order at room pressure and are expected to remain so even at higher pressures, the meeting point would be a simple *triple point*. (c) At pressures beyond the triple point, the col phase directly transforms to the Sm*C* phase. To our knowledge this is the first time such a transition has been observed.

Finally, we would like to make some remarks about the organization of the molecules in the cubic phase. In the compound studied here, the molecule has a strongly polar nitro group attached to one of the phenyl rings. But more importantly, there is a strong hydrogen bond network in the system due to the presence of carboxylic acid groups. X-ray investigations indicate that this network could be leading to the aggregation of the molecules, which in turn results in the appearance of the cubic phase [7,8,11,17–19]. As mentioned earlier, the analogy is quite striking in the nitro derivatives of the carboxylic acids, one of which is investigated in the present article, as it shows a phase sequence smectic-cubic-columnar mesophases. Based on the x-ray studies several structural models with different shapes and packing of the aggregation have been proposed. One such model is by Guillon and Skoulios [17], which we recall briefly here. This is a slight variation of the model proposed for lyotropic systems by Luzzati and Spegt [20]. According to this model, due to the carboxylic acid group the molecules form dimers and three such dimers lie side by side and in turn stack to form rods. Each end of the rod adjoins two others, the group of three rods being coplanar with the angle between the rods as 120°. In a feature that is pertinent to the compound that we have studied, due to the bulky nitro groups laterally sticking out of the molecules, it is argued that the dimers are stacked by rotating a little around the axis of the rod, forming a sort of helical superstructure. A similar model has been recently proposed by Kutsumizu *et al.* [12] to explain the infrared spectroscopy data on the nitro materials. We believe that it is the presence of the helical superstructure that is responsible for the drastic lowering of the relaxation frequency in the nitro compounds as compared with the data for the diols [6].

ACKNOWLEDGMENT

We are indebted to Professor S. Chandrasekhar for his keen interest in this work and for many useful discussions.

[1] See, e.g., S. Chandrasekhar, *Liquid Crystals* (Cambridge University Press, Cambridge, 1992).
[2] For a review, see J. M. Seddon and R. H. Templer, in *Handbook of Biological Physics*, edited by R. Lipowsky and E. Sackmann (Elsevier, Amsterdam, 1995), Vol. 1.
[3] G. W. Gray and J. W. Goodby, *Smectic Liquid Crystals-Textures and Structures* (Leonard Hill, Glasgow, 1984).
[4] K. Borisch, S. Diele, P. Göring, H. Kresse, and C. Tschierske, J. Mater. Chem. **8**, 529 (1998).
[5] For recent reviews, see S. Diele and P. Göring, in *Handbook of Liquid Crystals*, edited by D. Demus, J. Goodby, G. W. Gray, H. W. Spiess, and V. Vill (Wiley-VCH, Weinheim, 1998), and Ref. [4].
[6] H. Kresse, H. Schmalfuss, B. Gestblom, K. Borisch, and C. Tschierske, Liq. Cryst. **23**, 891 (1997).
[7] J. E. Lydon, Mol. Cryst. Liq. Cryst. Lett. **72**, 79 (1981).
[8] D. Demus, D. Marzotko, N. K. Sharma, and R. Wiegeleben, Krist. Tech. **15**, 331 (1980).
[9] G. W. Gray, B. Jones, and F. Marson, J. Chem. Soc. 393 (1957).
[10] D. S. Shankar Rao, V. K. Gupta, S. Krishna Prasad, M. Manickam, and S. Kumar, Mol. Cryst. Liq. Cryst. **319**, 193 (1998).
[11] A. M. Levelut and M. Clerc, Liq. Cryst. **24**, 105 (1998).
[12] S. Kutsumizu, R. Kato, M. Yamada, and S. Yano, J. Phys. Chem. **101**, 10 666 (1997).
[13] S. Havriliak and S. Negami, J. Polym. Sci., Part C: Polym. Symp. **14**, 99 (1966).
[14] S. Kutsumizu, M. Yamada, and S. Yano, Liq. Cryst. **16**, 1109 (1994).
[15] M. A. Anisimov, *Critical Phenomena in Liquids and Liquid Crystals* (Gordon and Breach, London, 1991).
[16] T. W. Stinson and J. D. Litster, Phys. Rev. Lett. **25**, 503 (1970); T. Stoebe, P. Mach, and C. C. Huang, *ibid.* **73**, 1384 (1994).
[17] D. Guillon and A. Skulios, Europhys. Lett. **3**, 79 (1987).
[18] P. Ukleja, R. E. Siatkowski, and M. E. Neubert, Phys. Rev. A **38**, 4815 (1988).
[19] G. Etherington, A. J. Leadbetter, X. J. Wang, G. W. Gray, and A. Tajbaksh, Liq. Cryst. **1**, 209 (1986).
[20] V. Luzzati and P. Spegt, Nature (London) **215**, 701 (1967).